Figures and figure supplements

Inactivation of *Invs/Nphp2* in renal epithelial cells drives infantile nephronophthisis like phenotypes in mouse

Yuanyuan Li and Wenyan Xu *et al*.

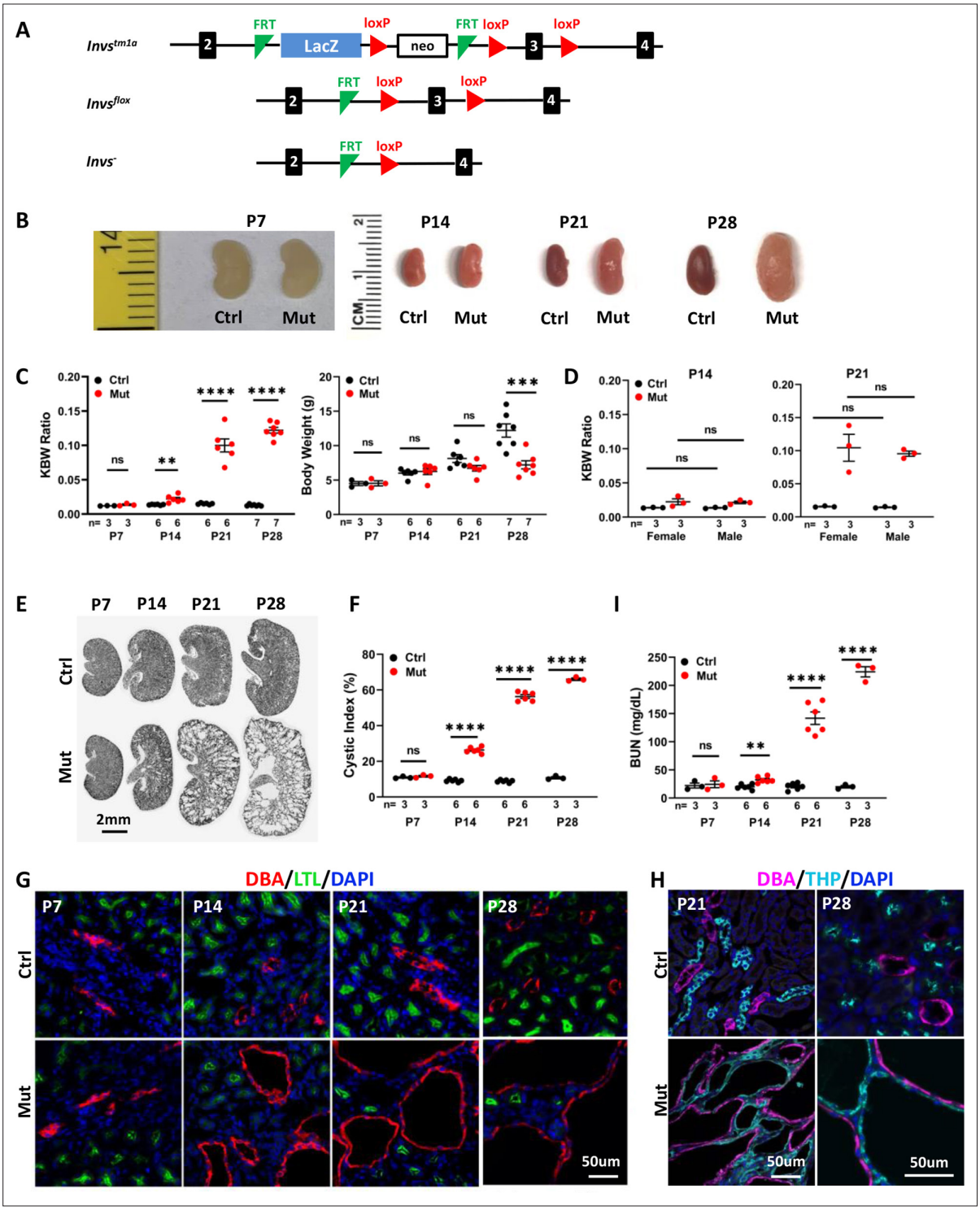

Figure 1. *Invs*$^{flox/flox}$*;Cdh16-Cre* mice develop progressive cystic kidney disease at the neonatal stage. (**A**) Generation of a floxed allele of *Invs*. FRT indicates FLPE recombinase sites, and loxP indicates Cre recombinase sites. (**B**) Gross morphology of the kidney. (**C**) KBW ratio and body weight in control and mutant mice. (**D**) KBW ratio in male and female mice. (**E**) HE-stained kidney sections. (**F**) Cystic index. (**G, H**) Origin of cysts. DBA marks the collecting duct in red in G and in purple in H. The proximal tubule is labeled with LTL in green and the medullary thick ascending limb is labeled by THP in cyan. Nuclei are labeled with DAPI in blue. (**I**) BUN level. Ctrl: littermate control; Mut: *Invs*$^{flox/flox}$*;Cdh16-Cre* mutants. Unpaired t-test was performed between mutants and control animals. Data are presented as mean ± SEM: ns: not significant (p>0.05); **: p<0.01; ***: p<0.001; ****: p<0.0001.

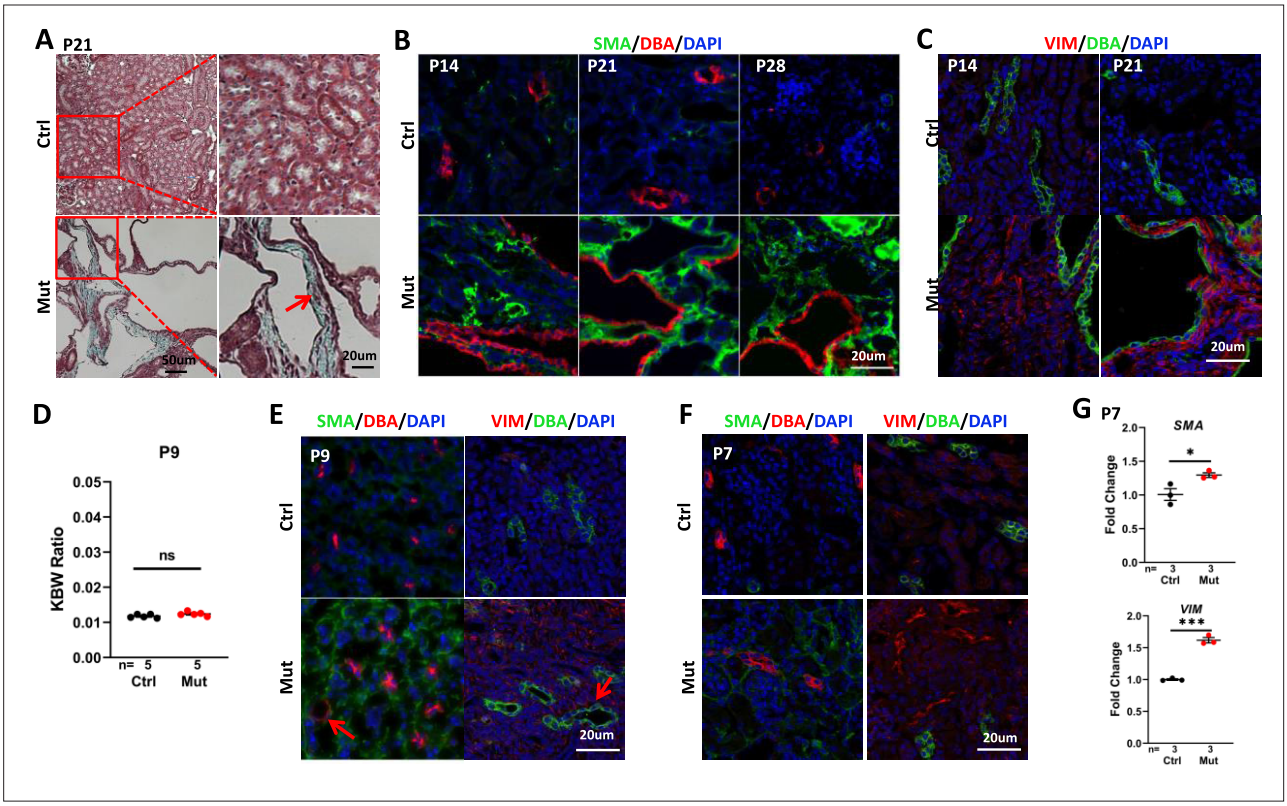

Figure 2. *Invs*$^{flox/flox}$*;Cdh16-Cre* mice develop interstitial fibrosis in the kidney. (**A**) Trichome staining of P21 kidney sections indicates blue collagen deposition (arrow) in the cortex region of a mutant kidney. (**B**) Increased signal of SMA (green) in the cortex region of mutant kidneys from P14 to P28. DBA in red marks the collecting duct. DAPI in blue labels the nucleus. (**C**) Increase of vimentin staining (VIM, red) in the cortex region of P14 and P21 mutant kidneys. DBA in green. DAPI in blue. (**D**) KBW ratio at P9. (**E, F**) Modest increase of SMA (in green, DBA in red in the left panels) and vimentin (VIM in red in the right panels, DBA in green) in the cortex region of the mutant kidney at P9 (**E**) and P7 (**F**). Arrows point to dilated tubules. DAPI in blue labels the nucleus. (**G**) The level of *SMA* (upper) and *Vimentin* (lower) mRNA is increased in the mutant kidney as assayed by RT-qPCR using P7 whole kidney lysates. Ctrl: littermate control; Mut: *Invs*$^{flox/flox}$*;Cdh16-Cre* mutants. Unpaired t-test was performed between mutants and control animals. Data are presented as mean ± SEM. ns: not significant (p>0.05); *: p<0.05; ***: p<0.001.

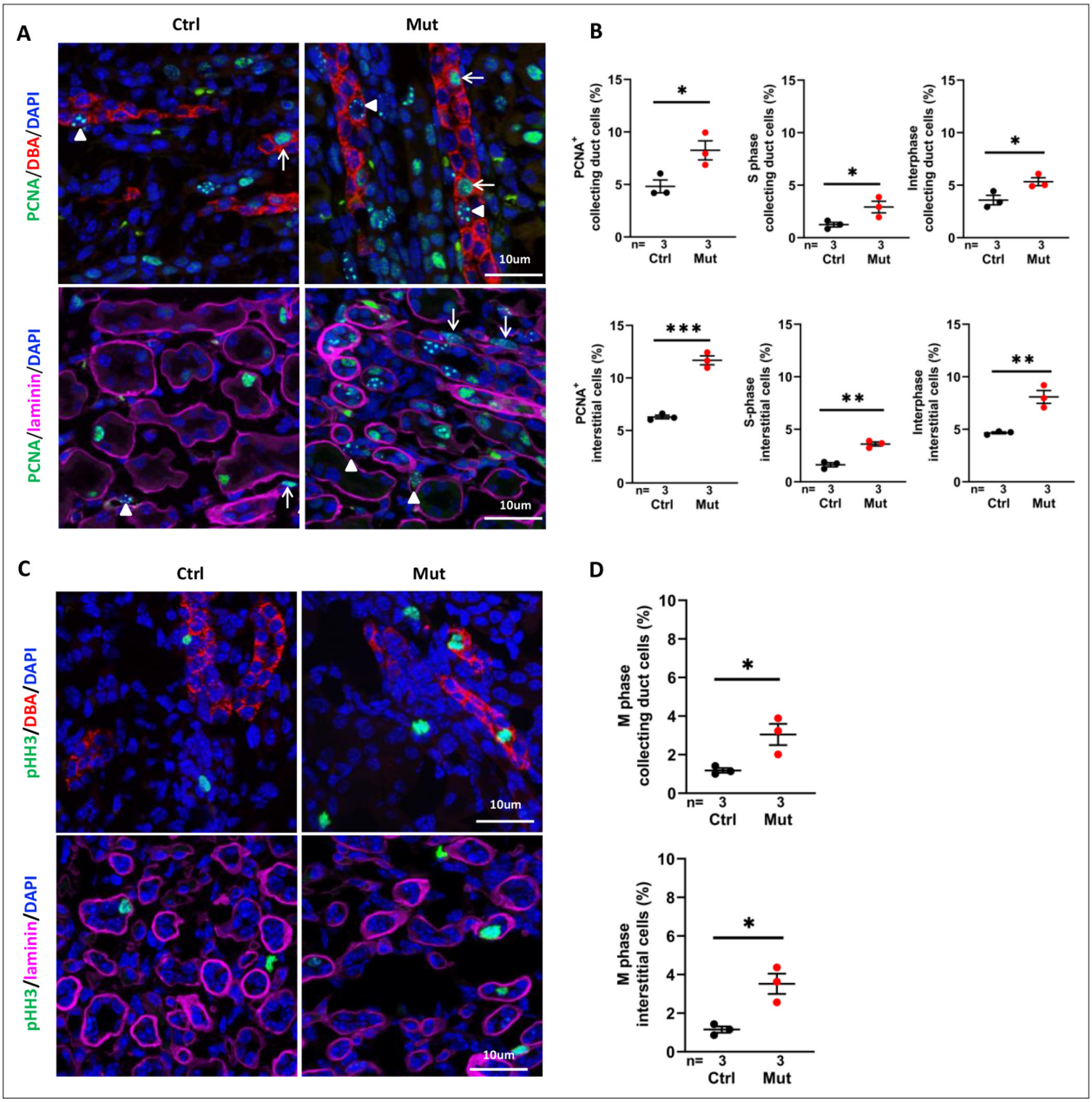

Figure 3. *Invs*$^{flox/flox}$*;Cdh16-Cre* kidneys show increased cell proliferation at P7. (**A**) Proliferating cells in the cortex region. PCNA (in green) stains replication foci in the nucleus of S-phase cells (examples pointed by arrowheads) but shows diffusive nuclear signal in interphase cells (arrows). In upper panels, collecting duct cells are labeled with DBA in red. In lower panels, epithelial regions are encircled by anti-laminin staining in purple. DAPI in blue labels the nucleus. (**B**) Percentage of total PCNA$^+$ cells, PCNA$^+$ S phase cells and PCNA$^+$ interphase cells in collecting duct cells and interstitial cells in the cortex region. (**C**) Mitotic cells labelled by anti-pHH3 in the cortex region. In upper panels, collecting duct cells are labelled with DBA in red. In lower panels, epithelial regions are encircled by anti-laminin staining in purple. (**D**) Percentage of mitotic cells in collecting duct cells (upper panel) and interstitial cells (lower panel) in the cortex region. DAPI in blue labels the nucleus. Ctrl: littermate control; Mut: *Invs*$^{flox/flox}$*;Cdh16-Cre* mutants. Unpaired t-test was performed between mutants and control animals. Data are presented as mean ± SEM. *: p<0.05; **: p<0.01; ***: p<0.001.

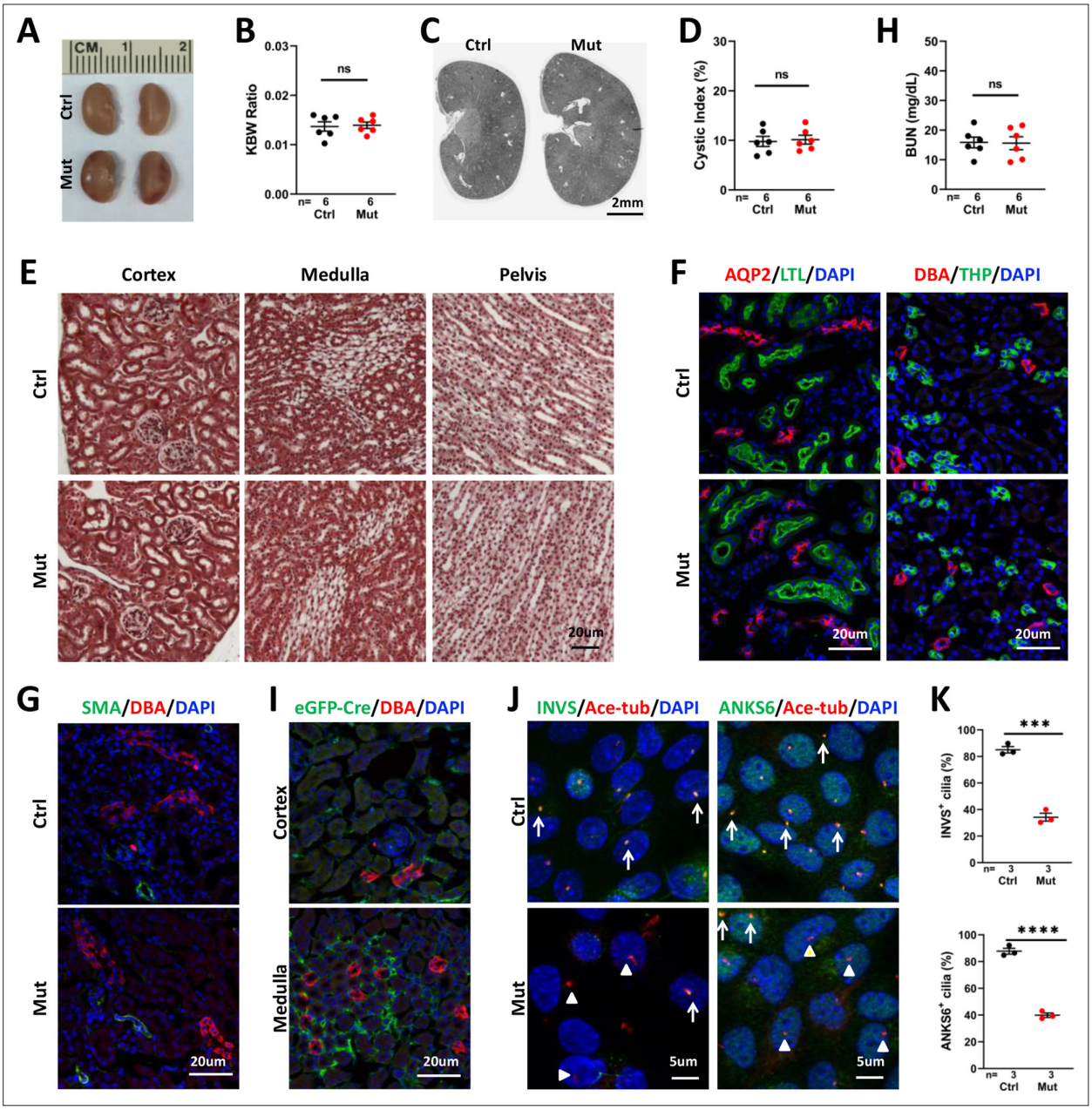

Figure 4. *Invs*$^{flox/flox}$*;Foxd1-Cre* kidneys show no significant phenotype at P28. (**A**) Gross morphology of the kidney. (**B**) KBW ratio. (**C**) HE-stained sections of the kidney. (**D**) Cystic index. (**E**) Trichrome staining of kidney sections. (**F**) Normal morphology of the collecting tubule and duct labelled by AQP2 (in red, left panels), collecting duct labelled by DBA (in red in right panels), proximal tubule (LTL in green in left panels) and thick ascending limb (THP in green in right panels). DAPI in blue labels the nucleus. (**G**) No increase of SMA signal (in green) can be detected in the mutant kidney. DBA in red labels the collecting duct. DAPI in blue labels the nucleus. (**H**) BUN level. (**I**) Immunostaining of eGFP-Cre (green). DBA in red. DAPI in blue. (**J**) Immunostaining of INVS (in green, left panels) and ANKS6 (in green, right panels) in primary culture of interstitial cells from control and mutant kidneys. Anti-acetylated tubulin (Ace-tub, red) labels cilia. DAPI in blue. Arrows indicate INVS or ANKS6 positive cilia. Arrowheads point to INVS^{-} or ANKS6^{-} cilia. (**K**) Quantification of INVS and ANKS6 positive cilia. Ctrl: littermate control; Mut: *Invs*$^{flox/flox}$*;Foxd1-Cre* mutants. Unpaired t-test was performed between mutants and control animals. Data are presented as mean ± SEM. ns: not significant (p>0.05); ***: p<0.001; ****: p<0.0001.

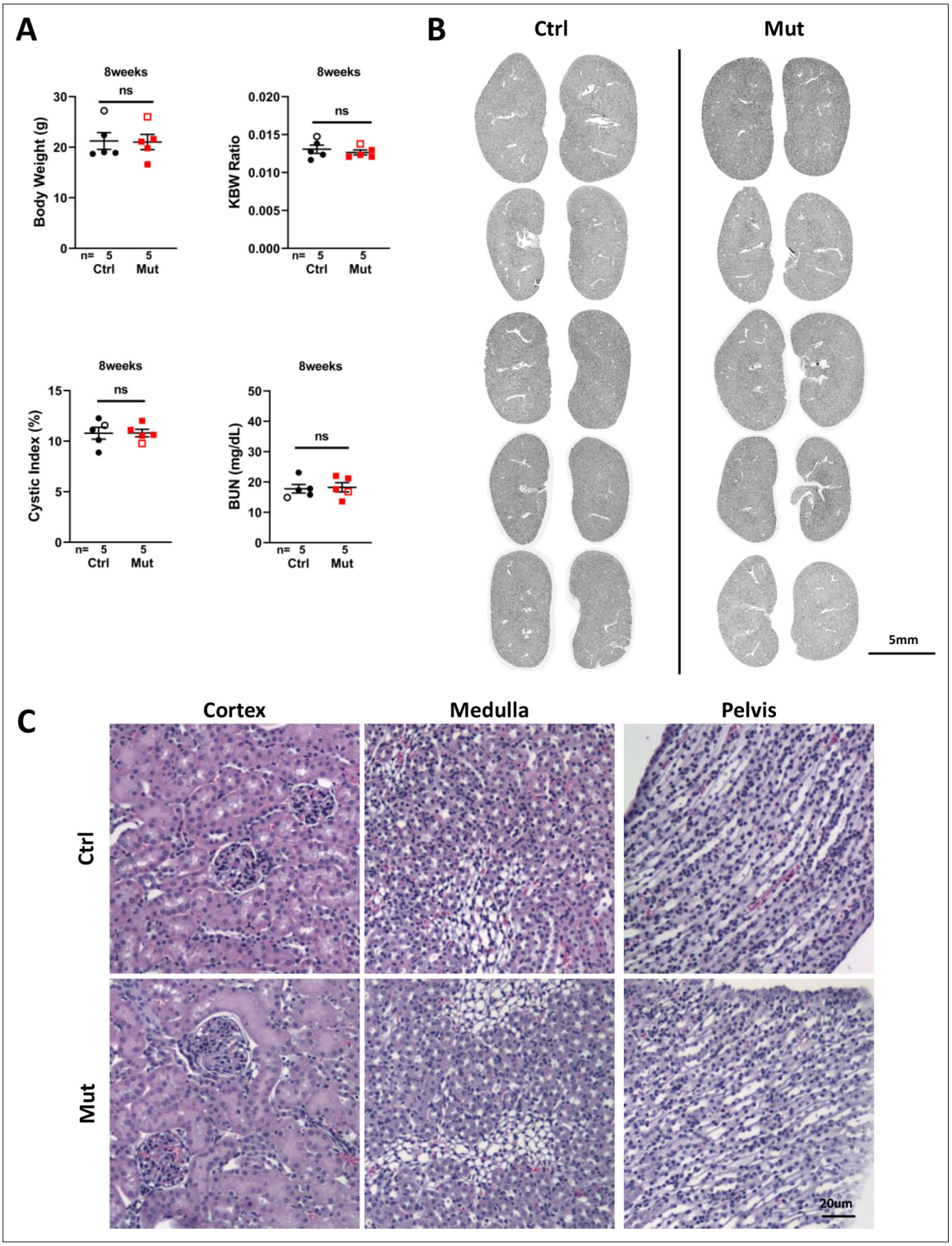

Figure 4—figure supplement 1. *Invs*$^{flox/flox}$*;Foxd1-Cre* kidneys show no significant phenotype at P56. (**A**) Body weight, KBW ratio, cystic index and BUN. Open labels indicate males and filled labels indicate females. (**B**) Section images of all kidneys analyzed in A. (**C**) Hematoxylin/eosin-stained sections of the kidney. Ctrl: littermate control; Mut: *Invs*$^{flox/flox}$*;Foxd1-Cre* mutants. Unpaired t-test was performed between mutants and control animals. Data are presented as mean ± SEM. ns: not significant (p>0.05).

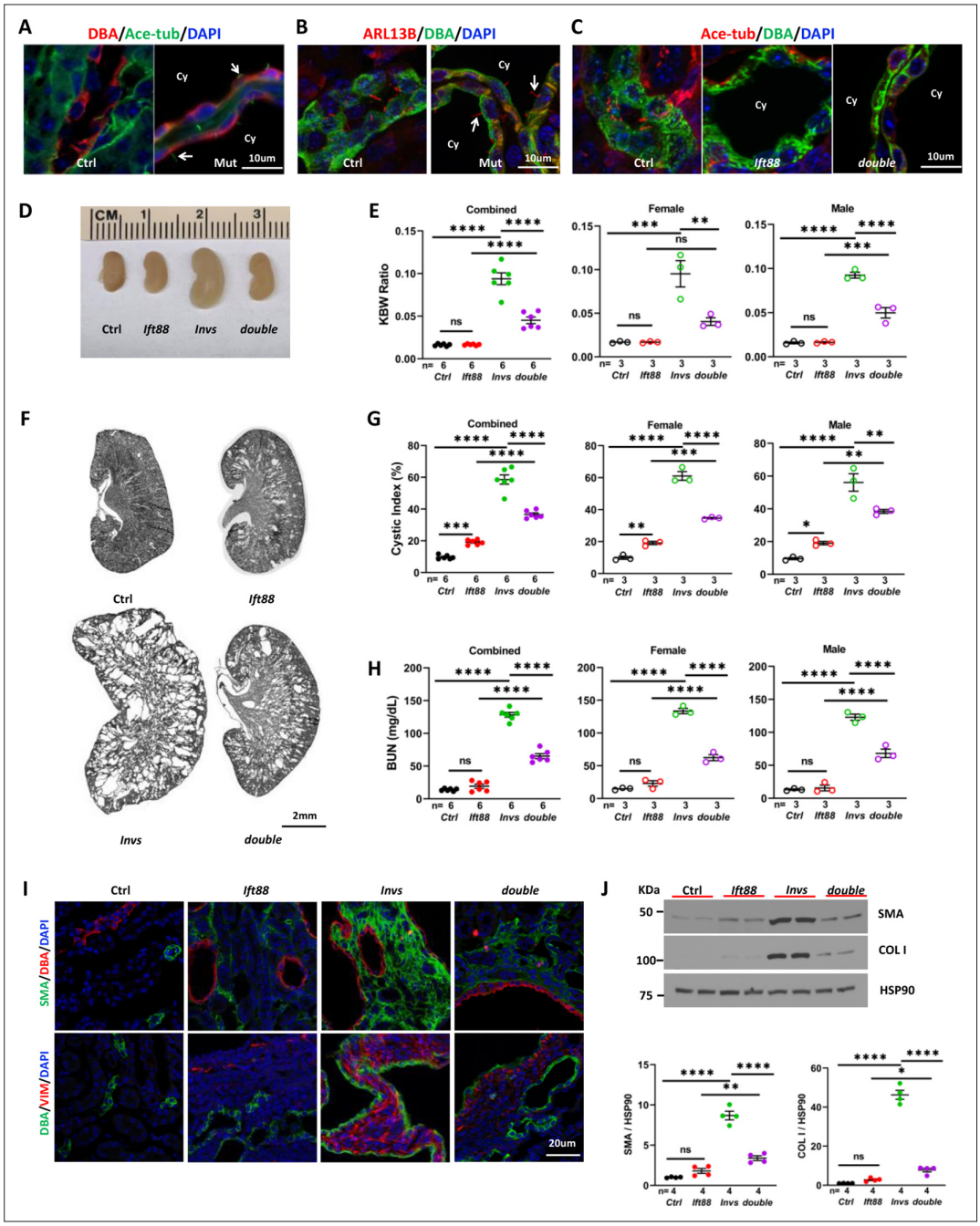

Figure 5. Genetic abrogation of cilia partially suppresses the phenotypes of *Invs*$^{flox/flox}$;*Cdh16-Cre* mice at P21. (**A**) *Invs* is dispensable for cilia biogenesis. Cilia (arrow) are labelled by anti-Ace-tub (green). The collecting duct is labeled by DBA (red). DAPI (blue) labels the nucleus. (**B**) *Invs* is dispensable for ciliary localization of ARL13b (red, arrow). DBA in green. DAPI in blue. (**C**) Cilia (labelled by anti-Ace-tub, red) biogenesis is disrupted in both *Ift88*$^{flox/flox}$;*Cdh16-Cre* knockout and *Invs*$^{flox/flox}$;*Ift88*$^{flox/flox}$;*Cdh16-Cre* knockout kidney. DBA in green. (**D**) Gross kidney morphology. (**E**) KWB ratio. (**F**) HE-stained kidney sections. (**G**) Cystic index. (**H**) BUN level. (**I**) Immunostaining of the renal cortex region. DBA in red and SMA in green in upper panels. DBA in green and vimentin (VIM) in red in lower panels. DAPI in blue. (**J**) Representative western blot and quantification. COL I: Collagen I. Ctrl: age matched controls from pooled litters; *Invs: Invs*$^{flox/flox}$;*Cdh16-Cre* mutant; *Ift88: Ift88*$^{flox/flox}$;*Cdh16-Cre* mutant; *double: Ift88*$^{flox/flox}$;*Invs*$^{flox/flox}$;*Cdh16-Cre* double mutant; Ace-tub: acetylated tubulin; Cy: cyst. One-way ANOVA analysis followed by Šidák's test was performed between selected pairs. Data are presented as mean ± SEM. ns: not significant (p>0.05); *: p<0.05; **: p<0.01; ***: p<0.001; ****: p<0.0001.

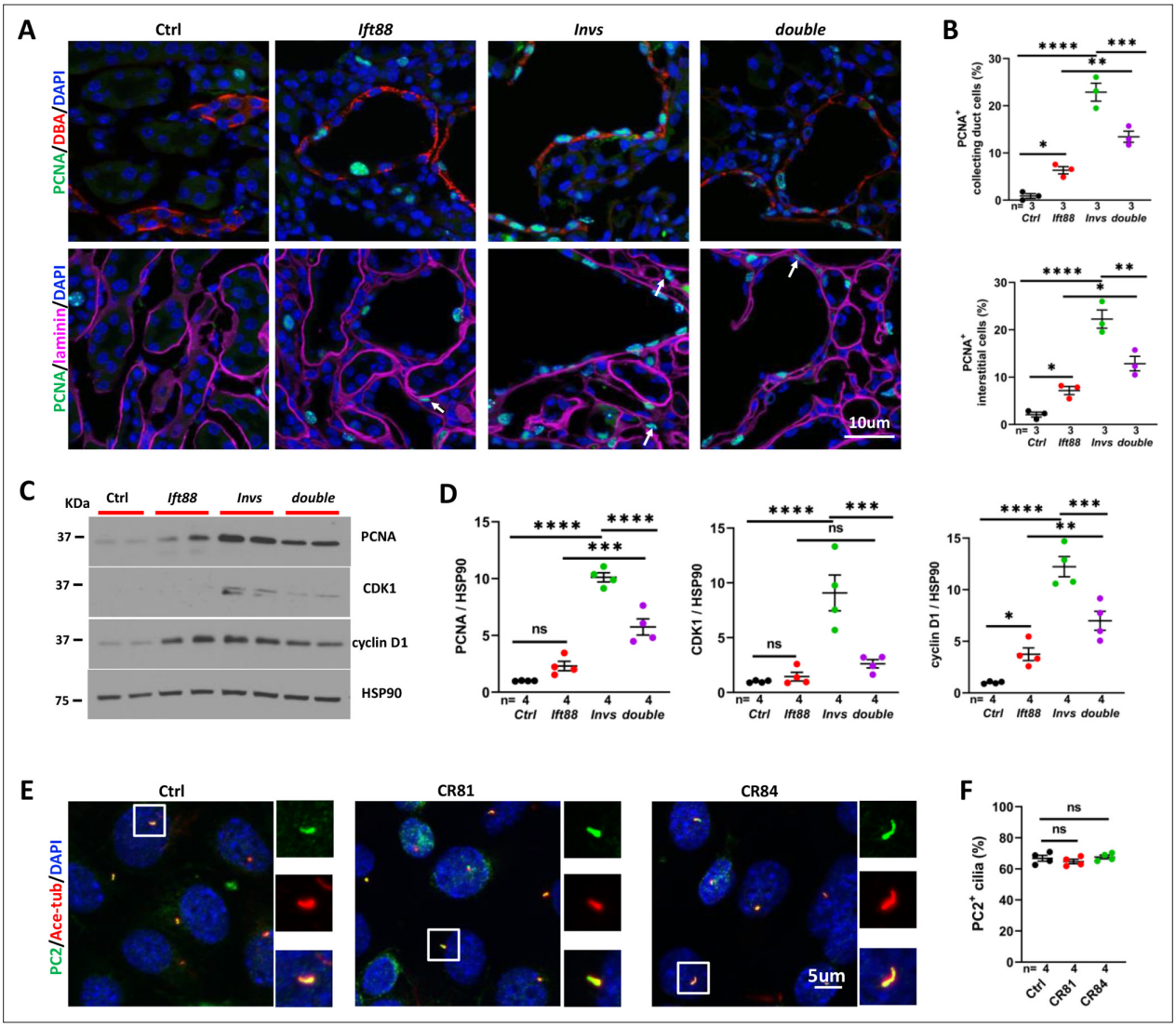

Figure 6. Genetic abrogation of cilia partially reduced cell proliferation in *Invs*$^{flox/flox}$;*Cdh16-Cre* kidney at P21. (**A**) PCNA (in green) staining of the cortex region. The collecting duct is labeled by DBA in red in upper panels. Epithelial regions are encircled by laminin signal in purple in lower panels. DAPI in blue labels the nucleus. Arrows point to representative PCNA^{+} interstitial cells. (**B**) Quantification of PCNA^{+} collecting duct cells (DBA) and interstitial cells outside of regions demarcated by laminin signal. (**C**) Representative Western Blot of PCNA, CDK1, cyclin D1 and the loading control HSP90 using kidney lysates. (**D**) Quantification of signals on Western Blots. Unit 1 is defined by the level in control kidneys. (**E**) Immunostaining of PC2 (in green) in control mIMCD3 cells (Ctrl) and mutant cells (Mut) from *Invs*$^{-/-}$ clones CR81 and CR84. Cilia are labeled by anti-acetylated tubulin (Ace-tub) in red. DAPI in blue labels the nucleus. (**F**) Quantification of PC2 positive cilia. *Invs: Invs*$^{flox/flox}$;*Cdh16-Cre* mutant; *Ift88: Ift88*$^{flox/flox}$;*Cdh16-Cre* mutant; *double: Ift88*$^{flox/flox}$;*Invs*$^{flox/flox}$;*Cdh16-Cre* double mutant. One-way ANOVA analysis followed by Šidák's test was performed between selected pairs. Data are presented as mean ± SEM. ns: not significant (p>0.05); *: p<0.05; **: p<0.01; ***: p<0.001; ****: p<0.0001.

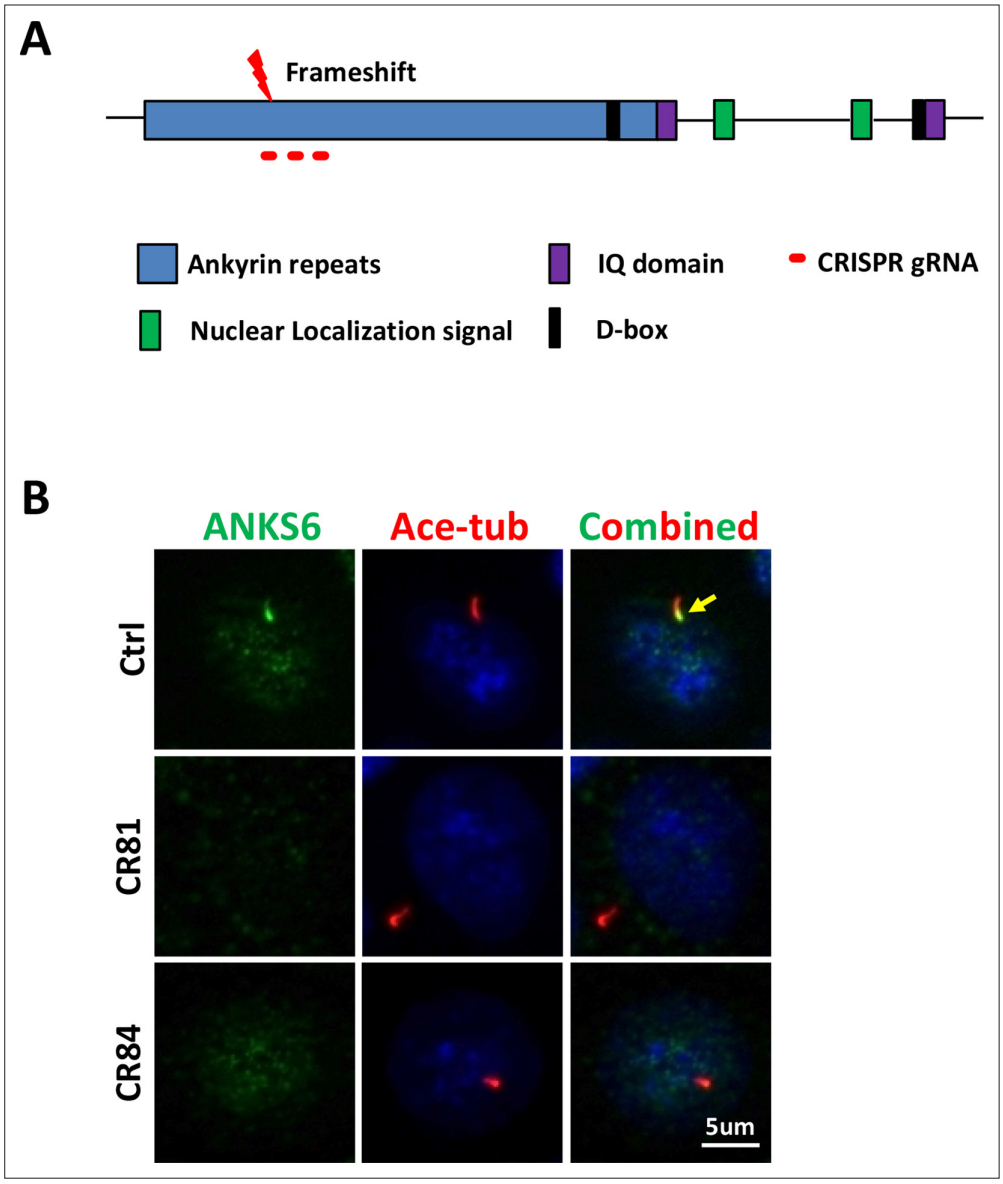

Figure 6—figure supplement 1. The generation of *Invs*$^{-/-}$ cells. (**A**) A diagram of INVS structure and CRISPR targets. (**B**) ANKS6 (green) is absent from the INVS compartment (arrow) of cilia. Cilia are labelled by anti-acetylated tubulin (Ace-tub, red) in mutant clones CR81 and CR84.

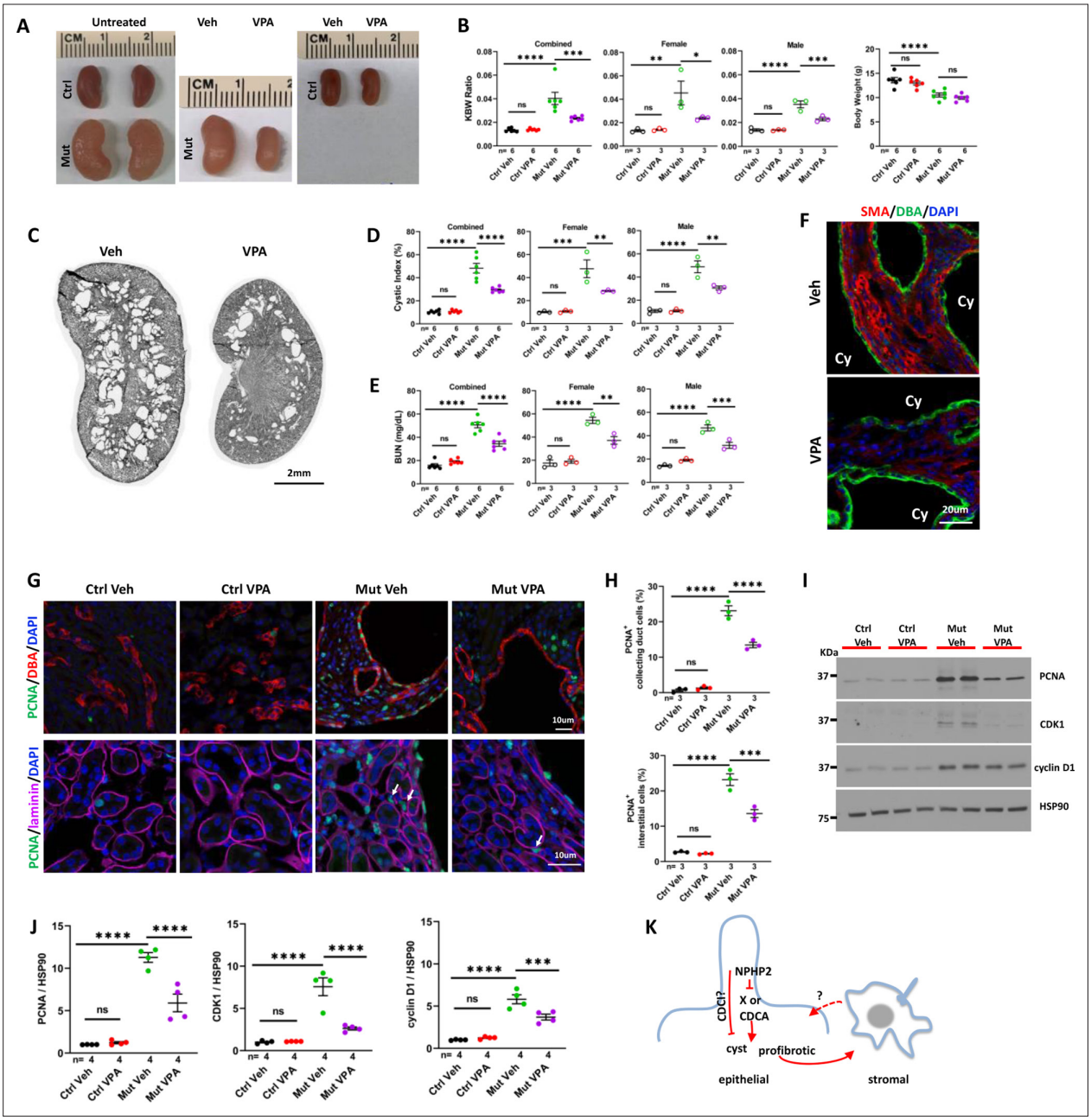

Figure 7. VPA partially suppresses the phenotypes of *Invs*$^{flox/flox}$*;Pkhd1-Cre* mice at P28. (**A**) Gross morphology of the kidney. (**B**) KBW ratio and body weight. (**C**) HE-stained kidney section. (**D**) Cystic index. (**E**) BUN level. (**F**) SMA (red) in the cortex region of the kidney. DBA in green marks the collecting duct. DAPI in blue labels the nucleus. (**G**) Proliferating cells labelled by anti-PCNA staining (in green) in the cortex region. In upper panels, DBA in red. In lower panels, anti-laminin staining in purple. Arrows point to representative PCNA^{+} interstitial cells. DAPI in blue. (**H**) Percentage of PCNA^{+} collecting duct cells (upper panel) and interstitial cells (lower panel) in the cortex region. (**I**) Representative western blot of PCNA, CDK1, cyclin D1 and the loading control HSP90. (**J**) Quantification of signals on western blots. (**K**) A model of INVS function. INVS in epithelial cilia inhibits a pro-cystic and profibrotic pathway, which activates interstitial cells non-cell autonomously. CDCI: cilia-dependent cyst inhibiting. Cy: cyst; Ctrl: age matched control animals from pooled litters; Mut: *Invs*$^{flox/flox}$*;Pkhd1-Cre* mutant; Veh: vehicle treated. One-way ANOVA analysis followed by Šidák's test was performed between selected pairs. Data are presented as mean ± SEM. ns: not significant (p>0.05); *: p<0.05; **: p<0.01; ***: p<0.001; ****: p<0.0001.

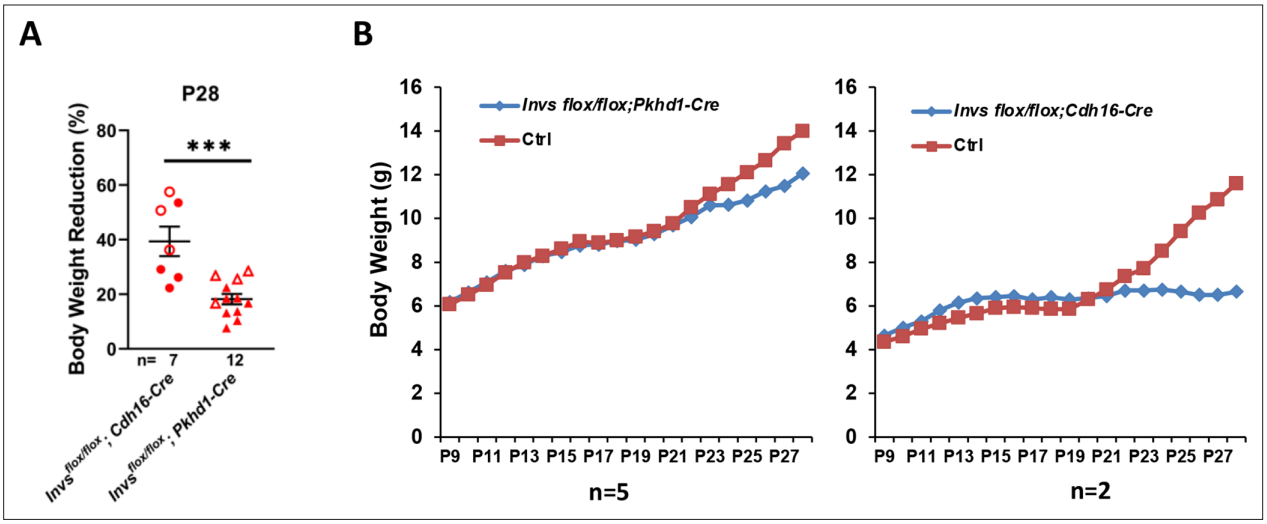

Figure 7—figure supplement 1. Body weight change of *Invs* models. (**A**) Decrease of body weight of *Invs*$^{flox/flox}$*;Cdh16-Cre* and *Invs*$^{flox/flox}$*;Pkhd1-Cre* at P28 compared to littermate controls. Percentage of body weight reduction is defined as the difference between littermate control and mutant body weight divided by littermate control body weight. Open labels indicate males and filled labels indicate females. (**B**) Average body weight curve of *Invs*$^{flox/flox}$*;Cdh16-Cre* and *Invs*$^{flox/flox}$*;Pkhd1-Cre* female mice. Ctrl: littermate control. Unpaired t-test was performed between mutants and control animals. Data are presented as mean ± SEM. ***: p<0.001.